Double-walled carbon nanotube array for CO_2 and SO_2 adsorption

Mahshid Rahimi, Deepu J. Babu, Jayant K. Singh, Yong-Biao Yang, Jörg J. Schneider, and Florian Müller-Plathe

Citation: J. Chem. Phys. **143**, 124701 (2015); doi: 10.1063/1.4929609
View online: http://dx.doi.org/10.1063/1.4929609
View Table of Contents: http://aip.scitation.org/toc/jcp/143/12
Published by the American Institute of Physics

Double-walled carbon nanotube array for CO_2 and SO_2 adsorption

Mahshid Rahimi,[1,a),b)] Deepu J. Babu,[1,b)] Jayant K. Singh,[1,2] Yong-Biao Yang,[1] Jörg J. Schneider,[1,a)] and Florian Müller-Plathe[1]
[1]*Eduard-Zintl-Institut für Anorganische und Physikalische Chemie, Technische Universität Darmstadt, Alarich-Weiss-Str. 4, D-64287 Darmstadt, Germany*
[2]*Department of Chemical Engineering, Indian Institute of Technology Kanpur, Kanpur 208016, India*

(Received 26 March 2015; accepted 20 July 2015; published online 22 September 2015)

Grand-canonical Monte Carlo simulations and adsorption experiments are combined to find the optimized carbon nanotube (CNT) arrays for gas adsorption at low pressures and 303 K. Bundles of 3D aligned double-walled carbon nanotube (DWCNT) with inner diameter of 8 nm and different intertube distances were made experimentally. The experimental results show that decreasing intertube distance leads to a significant enhancement in carbon-dioxide (CO_2) adsorption capacity at 1 bar. The molecular simulation study on CO_2 adsorption onto bundles of 3D aligned DWCNT with inner diameters of 1, 3, and 8 nm and intertube distance of 0-15 nm shows that the intertube distance plays a more important role than the CNT diameter. The simulation results show that decreasing the intertube distance up to 1 nm increases the excess adsorption generally in all the studied systems at pressures $0 < p < 14$ bars (the increase can be up to ~40% depending on the system and pressure). This is in agreement with the experimental result. Further reduction in intertube distance leads to a decrease in the excess adsorption in the pressure range $9 < p < 14$ bars. However, at lower pressure, $0 < p < 9$ bars, intertube distance of 0.5 nm is found to have the highest excess adsorption. This result is indifferent to tube diameter. Furthermore, molecular simulations are conducted to obtain the optimal parameters, for the DWCNT bundle, for SO_2 adsorption, which are similar to those observed for CO_2 in the pressure range $0 < p < 3$ bars. © *2015 AIP Publishing LLC.* [http://dx.doi.org/10.1063/1.4929609]

I. INTRODUCTION

In the previous decade, carbon-dioxide (CO_2) emissions from the combustion of fossil fuels (coal, petroleum, and natural gas) accounts for 78% increase of greenhouse gases in the atmosphere.[1] Annual emissions of greenhouse gases, specially CO_2, are the main cause of the global warming.[2] Among other gases emitted from fossil fuel combustion, SO_2 contributes significantly in polluting the environment. It is one of the major reasons of acid rain formation.[3] The main strategy for a solution for these environmental concerns is to find a suitable material for capture and storage of these gases.

Carbon based materials are widely used for gas adsorption because of the preferential interaction that exists between gas molecules and carbon atoms.[4] Carbon nanotubes (CNTs) are an important class of carbon based materials. Due to their unique structure, CNTs have extraordinary mechanical, electrical, and thermal properties.[5] Recently, a new interest on them arose because of their potential as an adsorbent of flue gases. Their large specific area, light weight, well defined structure, and reproducibility are the properties that make them one of the most promising carbon based adsorbents.[6–8] Since CNTs are well-defined structures, optimizing their geometrical properties is very important to achieve the maximum possible amount of adsorption. Liu and co-workers[9] used grand-canonical Monte Carlo (GCMC) technique to study CO_2 adsorption on single-walled CNT (SWCNT) with different chiralities, and two different diameters, 1.36 and 2.03 nm, at 300 K. They found that the adsorption capacity of SWCNT could be enhanced by the increase in the SWCNT diameter while chirality is not an essential factor on adsorption. Using the same method to investigate different gases ($CO_2/CH_4/N_2/H_2/CO$) adsorption on hexagonally ordered carbon nanopipes at 298 K, Peng *et al.*[10] claimed that increasing pore diameter from 3 to 6 nm leads to an increase in pure gases adsorption, especially for CO_2. Kowalczyk *et al.*[11] studied the effect of SWCNT diameter on the CO_2 storage at 298 K using GCMC method. They claimed that the optimum diameter of CNT depends on the storage pressure.

Usually, CNTs form bundles or undergo complex aggregation, depending on the process of synthesis. Cao *et al.*[12] and Zilli *et al.*[13] experimentally showed that aligned CNTs have higher adsorption capacity. A combined study of molecular simulation and experiment of nitrogen adsorption was performed by Agnihotri *et al.*[14] to explain the high capacity of CNT bundles. They showed that CNT bundles exhibit different sites, namely, inner (the volume within the tubes), grooves (where the two CNTs are in touch), and interstitial (the region surrounded by three CNTs and three grooves). The groove regions play an important role on adsorption at low pressure till they are saturated. Cruz *et al.*[15] used GCMC to study light organic adsorption in the internal volume of SWCNT bundles and external adsorption sites separately at 300 K. In the case of external adsorption sites, they observed that the adsorption is

a)Author to whom correspondence should be addressed. Electronic addresses: mahshid.rahimi@theo.chemie.tu-darmstadt.de and joerg.schneider@ac.chemie.tu-darmstadt.de
b)M. Rahimi and D. J. Babu contributed equally to this work.

higher in grooves. Furthermore, they found that adsorption in grooves is in agreement with the Langmuir adsorption model.

Although many works confirmed that interstitial region and grooves are important adsorption sites,[16–20] not much is known about the optimal intertube distance for highest adsorption capacity of CNT bundles. Furthermore, the effect of curvature due to variable double-walled carbon nanotube (DWCNT) diameter, on the optimal intertube distance, was missing in the earlier works. In the present work, we study SO_2 and CO_2 adsorption onto DWCNT bundles with different diameters and intertube distances. The aim is to optimize diameter and intertube distance of DWCNT bundles for the maximum adsorption capacity at low pressures. Besides, a comparison is performed with the previous works of this group.[21,22]

II. EXPERIMENTAL DETAIL

Vertically aligned CNTs were synthesized by water assisted CVD method. In a typical synthesis, 10–13 nm of Al was deposited onto boron doped Si/SiO_2 (600 nm of SiO_2) substrate by thermal evaporation method. This was followed by the deposition of 1.2 nm of iron by sputtering. The substrate along with deposited catalyst was transferred to a 3 in. CVD quartz tube and was heated to 850 °C under a reducing atmosphere. Ethene was used as the carbon source and synthesis was carried out for 15 min in the presence of controlled ppm quantities of water. Further details can be found elsewhere.[23] Densification of CNT arrays was carried out by using ethanol (technical grade) or deionized water. CNT films were peeled off from the substrate and a few drops of ethanol or water were placed on top of these films. The liquid was left to evaporate overnight at room temperature.

CO_2 adsorption measurements were carried out using a TG setup (TG209F1 Iris, Netzsch GmbH). Gas inlet was controlled using a mass flow controller gas flow meter (Bronkhorst High-Tech B.V.). About 10 mg of CNTs was placed in a ceramic crucible and was heated to 300 °C under 50 SCCM of argon flow. After maintaining the sample at 300 °C for 2 h, it was cooled down to 35 °C and kept at this temperature for half an hour. The gas supply was then switched from argon to 50 SCCM of CO_2 for an hour. After the adsorption step, the sample was again heated to 300 °C in argon. A reference measurement, without the sample, was carried out before each measurement to account for buoyancy corrections. SEM measurements were carried out on a Philips XL30 FEG. N_2 adsorption measurements were performed on a quantachrome autosorb® system. About 30 mg of sample was used for each measurement and was evacuated overnight at a temperature of at least 250 °C. Specific surface areas were calculated using a multi-point BET method.

III. MODEL AND METHOD

Following our previous work, we arrange double-walled CNTs on a hexagonal lattice so that two CNTs are in a periodic simulation box (cf. Fig. 1 of Ref. 19). In order to study the effect of curvature and porosity of the system, armchair CNTs with the inner diameter of $2r$ = 1, 3, 8 nm, a length of 5 nm, and the intertube distances of d = 0 to 15 nm are used in this work. The total number of carbon atoms is between 3360 and 19 680, depending on the CNT diameter.

SO_2 and CO_2 molecules are modeled using a 3-site rigid model with Lennard-Jones potential, partial charges, and fixed angle.[24,25] We describe CNTs as rigid structure with Lennard-Jones potential as in AMBER96 force field.[26] The Lorentz-Berthelot combining rules are used to calculate the dissimilar non-bonded interactions. The electrostatic interactions are calculated by the smooth-particle-mesh Ewald (SPME) method.[27]

Excess adsorption isotherms of CO_2 and SO_2 are calculated using GCMC method at a constant chemical potential μ, volume V, and temperature T. In order to transform the chemical potential to pressure, CO_2 and SO_2 are considered as ideal gases since the fugacity coefficient of them is ~1 in the studied pressure range. Three Monte Carlo moves, displace, rotate, and insert/delete are implemented with the probability of 0.2, 0.1, and 0.7, respectively. For equilibration of the system, 10^7 Monte Carlo steps are used and then the simulation continues for another 10^7 steps to collect the data. The output of the simulation is the total number of gas molecules, N_{tot}, which varies between 80 and 3000 for CO_2 and between 85 and 3600 for SO_2 for different systems and pressures. Total number of gas molecules, N_{tot}, can be converted to excess adsorption (the value measured in experiment) by

$$N_{ex} = N_{tot} - \rho_b V_{free}, \tag{1}$$

where ρ_b is the bulk density and is calculated by simulating bulk fluid at the same condition. Free volume, V_{free}, is calculated using a 3-dimentional Monte Carlo integration as explained in the work of Greenfield and Theodorou.[28] The free volume in different system varies from 7.32 nm^3 to 2461.74 nm^3. We convert the unit of excess adsorption to a common unit for excess adsorption, mmol of gas per gram of adsorbent.

In an adsorption process, the isosteric heat of adsorption, q_{st}, which reflects the strength of adsorbent-adsorbate interaction,[29] is usually calculated by[30]

$$q_{st} \approx RT - \left(\frac{\partial U_{ad}}{\partial N_{ad}}\right)_{T,V}, \tag{2}$$

where R is the gas constant and U_{ad} is the intermolecular energy of the system. Using fluctuation theory, Eq. (2) can be written as

$$q_{st} \approx RT - \frac{\langle U_{ad}N_{ad}\rangle - \langle U_{ad}N_{ad}\rangle}{\langle {N_{ad}}^2\rangle - \langle N_{ad}{}^2\rangle}, \tag{3}$$

where the angle brackets denote the ensemble average.

IV. RESULTS AND DISCUSSION

A. Experimental results of CO_2 adsorption

In our previous works, we have carried out extensive characterization of the as-prepared aligned CNTs which are the sole material used in this study.[22,31,32] The as-synthesized double walled CNTs, containing a minor amount of multi-walled CNT (number of walls ≤4), have an average diameter of about 8 nm[22,31] and a height of 500 μm. Typical intertube distances (d) of the as-prepared vertically aligned structures

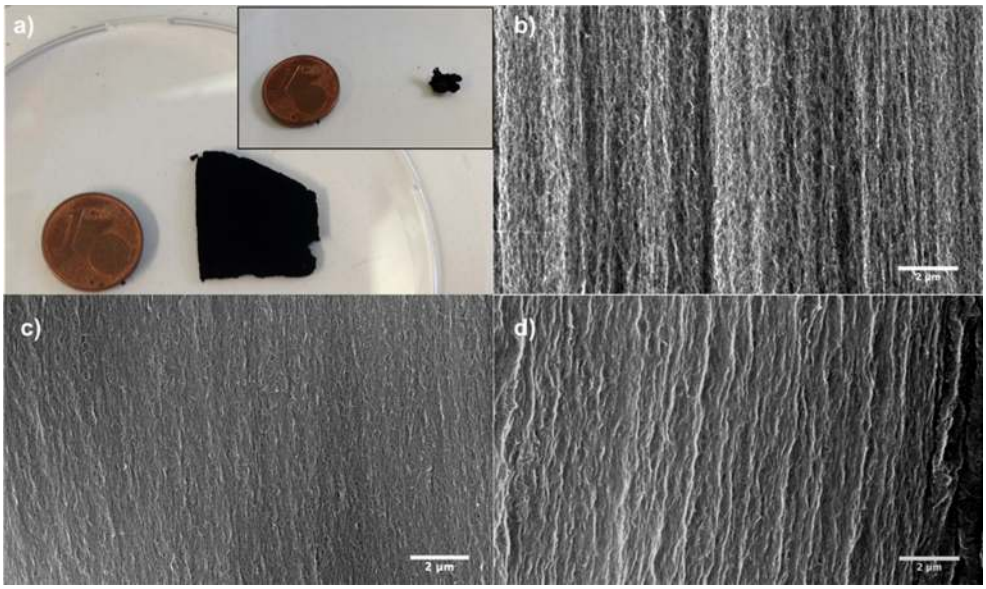

FIG. 1. (a) Photograph of the as-prepared vertically aligned CNT structure; inset shows the photograph of the same structure after ethanol evaporation. SEM images of (b) as-prepared vertically aligned CNT, (c) densified CNT by ethanol evaporation, (d) densified CNT architecture obtained by water evaporation (scale bar = 2μm).

are between 15 and 20 nm.[22] XPS measurements of the aligned CNTs indicated no peaks other than carbon (C1s), ruling out the presence of catalyst particles or functional groups in the as-prepared CNT.[22,31,32] Our previous CO_2 adsorption studies on these pristine CNT structures revealed an adsorption capacity of about 5.6 mg/g at 1 bar and 35 °C.[22] Theoretical calculations have shown that the interstitial sites are energetically favorable for adsorption and the adsorption capacity can be increased by optimizing the intertube distance.[21] To validate these results, all other parameters such as CNT diameter and specific surface area have to be kept constant and only the intertube distance should be varied. This can be realized by varying the bimetallic catalyst density. However, this invariably also leads to structural changes in CNT diameter as well as specific surface area.[33,34] Herein, we use the elastocapillary phenomenon[35] (also known as liquid induced collapse[36]) to increase the active surface area of the vertically aligned CNTs. When a liquid is introduced in the CNT arrays and allowed to evaporate, the resulting capillary and van der Waals forces effectively "zip" the nanotubes together, thereby densifying the structure. Futaba *et al.*[36] have shown that for aligned SWNT arrays, the intertube distance could be brought down from 15 nm to less than 1 nm without reducing the surface area. In the present study, we used ethanol and water for densification of vertically aligned CNT arrays. The CNT film crumbled upon evaporation and a considerable reduction in sample area is observed as shown in Fig. 1(a). Figs. 1(b)-1(d) show the SEM images of vertically aligned CNT structures before and after densification by elastocapillarity. The intervoid space between individual CNTs is considerably reduced after liquid evaporation. Though the macroscopic structure of the film is visibly distorted, the microscopic alignment is still intact to a certain degree. From SEM images, it is hard to discern differences between ethanol (Fig. 1(c)) and water (Fig. 1(d)) induced densified structures. However, CO_2 adsorption measurements revealed a significant difference between the two obtained CNT morphologies. Ethanol intercalated structures adsorbed about 7.5 mg/g of CO_2 at 1 bar/35 °C, whereas water intercalated CNT structures adsorbed 8.8 mg/g as shown in Fig. 2(a). This corresponds to an increase of 34% and 57% for ethanol and water intercalated

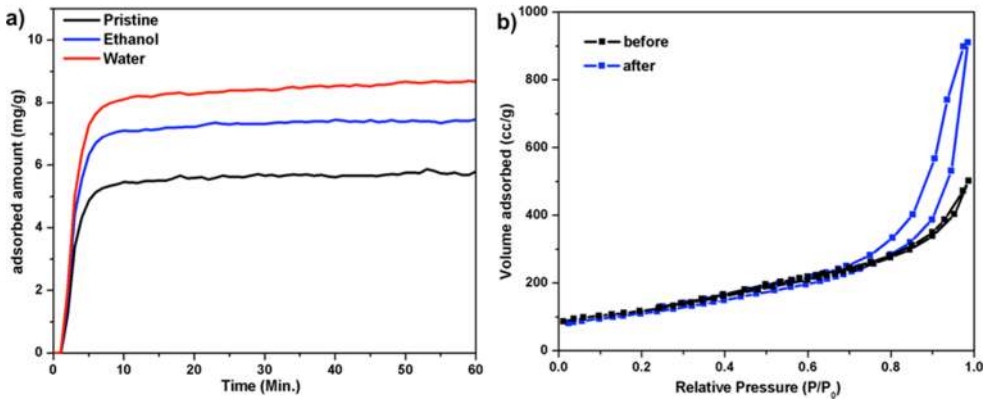

FIG. 2. (a) CO_2 adsorption at 1 bar and 35 °C for pristine and densified CNT structures. (b) N_2 adsorption isotherm on CNT structures before and after ethanol induced densification.

CNT architectures, respectively. De Volder and Hart[35] have shown that for a given material and geometry, the liquid induced compaction is proportional to the surface tension of the liquid. Water has a considerably higher surface tension of 71.99 m Nm^{-1} compared to 21.97 m Nm^{-1} of ethanol at 25 °C.[37] This may account for the better compaction and the observed enhancement in CO_2 adsorption for water intercalated structures.

N_2 adsorption measurements were carried out at 77 K before and after ethanol induced densification as shown in Fig. 2(b). No considerable changes in specific surface area are observed after the liquid induced collapse. Prior to densification, the CNT arrays had a BET specific surface area of about 423 m^2/g and after the evaporation of ethanol, the surface area decreased only slightly to 400 m^2/g. Similar observation regarding surface area was also made by Futaba *et al.* after densification of SWNT arrays.[36] From the N_2 adsorption isotherm, it can be observed that for the densified structure, the onset of capillary condensation (steep rise in adsorption) occurs at a lower pressure when compared to original structure. CO_2 adsorption on the densified structure clearly indicated an increase in the adsorption at 1 bar as shown in Fig. 2(a). In order to obtain the optimized value of the intertube distance, molecular simulation is used comprehensively to study the CO_2 adsorption on DWCNT bundles, which is described in detail in Sec. IV B.

B. Molecular simulation of CO_2 adsorption

Fig. 3 shows the CO_2 adsorption isotherms on DWCNT bundles with inner diameter $2r = 1$ nm and intertube distance $d = 0$-15 nm at $T = 303$ K. By increasing d, the volume of the grooves increases leading to decrease in the adsorptivity of the carbon surface. Hence, the propensity for adsorption is higher at lower values of d. However, at low d, the groove volume is limited which saturates at a lower pressure, and at higher pressures, the amount of adsorption for the larger groove volume exceeds the amount seen for lower d values. Hence, the optimal intertube distance varies for a given pressure range depending on the above two opposite effects (increase in volume and decrease in carbon density). The system with $d = 0$ reaches the saturation value of ~2 mmol/g at a low pressure ($p < 1$ bar), due to its limited space in the intertube region. Increasing d to 0.5 nm increases the excess adsorption significantly (e.g., 125% at $p = 1$ bar and 250% at $p = 4$ bars). Nevertheless, the isotherm saturates at $p \sim 8$ bars and the adsorption amount remains almost constant (~9 mmol/g) at higher pressure. The excess adsorption of $d = 1$ nm is less than that of $d = 0.5$ nm in the low pressure range $0 < p < 9$ bars. This is primarily due to increase in the DWCNT surface-surface distance with increase in d leading to reduction in the carbon density in the grooves. This affects the effective interaction experienced by a gas molecule that decreases with increase in d. Hence, the saturation occurs at a higher pressure and this is the reason that $d = 1$ curve crosses $d = 0.5$ nm curve at $p \sim 9$ bars. Further increase in d to 2, 4, and 15 nm decreases the excess adsorption in the studied pressure range, so that these three cases show fairly similar curves. When $d = 0.5$ nm, the grooves have low volume but they have a very high adsorptivity due to the high carbon density in these regions. Thus, $d = 0.5$ nm shows the highest adsorption at low gas pressure; then, with increasing pressure, it saturates. By increasing d to 1 nm, the groove regions become larger but at the same time, larger space decreases the carbon density and the adsorptivity. Consequently, at low pressure, it shows lower adsorption than that of $d = 0.5$ nm but at higher pressure, where $d = 0.5$ nm saturates, adsorption for the case $d = 1$ nm becomes more than that of $d = 0.5$ nm.

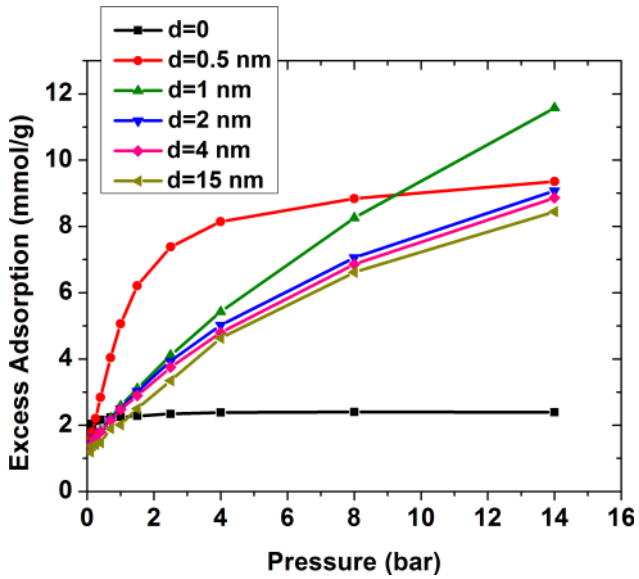

FIG. 3. Excess adsorption isotherms of CO_2 in double-walled carbon nanotube arrays, with inner tube diameter $2r = 1$ nm and intertube distance $d = 0$-15 nm. $T = 303$ K. Error bars are smaller than the symbols.

In order to understand the adsorption behavior of CO_2 and SO_2 on the CNT bundles, Langmuir and Freundlich adsorption models are used in this work. The Langmuir adsorption model[38] can explain the monolayer adsorption behavior with the following equation:

$$N_{ex} = N_{ex}^{max} \frac{bp}{1 + bp}, \tag{4}$$

where b is the Langmuir constant, p is the pressure, and N_{ex}^{max} is the maximum CO_2 loading. Freundlich adsorption model[39] is another popular model, which relates excess adsorption to the pressure,

$$N_{ex} = Kp^n, \tag{5}$$

where K is Freundlich constant and shows the adsorption capacity, n is heterogeneity factor, and p is the pressure. The above models are fitted to the GCMC data of CO_2, and the results are summarized in Table I. The worst and best fits of the Langmuir model are for $d = 0$ nm and $d = 0.5$ nm, respectively (see Fig. S1 of the supplementary material[40]). As the intertube distance increases, the fit of the Langmuir model gets relatively inaccurate as reflected by R^2. On the other hand, worst fit for the Freundlich model is for $d < 1.0$ nm, whereas the fit is excellent for all intertube distances $d \geq 1$ nm (see Fig. S2 of the supplementary material[40]). Thus, for $d \geq 1$ nm, Freundlich isotherm fits much better than the Langmuir isotherm. Hence, it is clear that for higher intertube distance, $d \geq 1$ nm multilayer

TABLE I. Langmuir and Freundlich isotherm parameter obtained by fitting for CO_2 adsorption on double-walled CNT with $2r$ = 1 nm and d = 0-15 nm. R^2 is the coefficient of determination of fitting.

	Langmuir model			Freundlich model		
d	N_{ex}^{max}	b	R^2	K	n	R^2
0	2.35 ± 0.02	45.43 ± 6.00	0.88	2.23 ± 0.01	0.04 ± 0.00	0.92
0.5	9.92 ± 0.22	1.10 ± 0.08	0.99	4.66 ± 0.31	0.31 ± 0.04	0.91
1	16.03 ± 2.36	0.15 ± 0.05	0.94	2.68 ± 0.13	0.55 ± 0.02	0.99
2	10.56 ± 1.21	0.29 ± 0.08	0.92	2.69 ± 0.08	0.46 ± 0.01	0.99
4	10.33 ± 1.26	0.28 ± 0.08	0.91	2.61 ± 0.09	0.46 ± 0.02	0.99
15	10.66 ± 1.34	0.22 ± 0.06	0.93	2.31 ± 0.11	0.49 ± 0.02	0.98

adsorption behavior is observed. The multilayer adsorption behavior of the system with $d > 1$ nm is also confirmed by the simulation snapshots (see Fig. S3 of the supplementary material[40]). The table clearly shows the remarkable effect of d on the adsorption capacity. Further, it is evident that d = 1 nm has the highest N_{ex}^{max} and n, i.e., d = 1 nm has the maximum capacity for CO_2 adsorption (62% and 52% more than d = 0.5 and 2 nm, respectively).

Figs. 4(a) and 4(b) present CO_2 adsorption on DWCNT with $2r$ = 3, 8 nm and various intertube distances. The intertube distance of d = 4 and 15 nm is not included as adsorption behavior seen for them is akin to that seen for d = 2 nm. The effect of intertube distance is more or less the same for different diameters. The adsorption behavior is not much different from that of $2r$ = 1 nm. At low pressure, $p < 9$ bars, d = 0.5 nm has the highest excess adsorption while at high pressure, $p > 9$ bars, the maximum excess adsorption belongs to d = 1 nm. The effect of intertube distance, however, reduces with increasing DWCNT diameter. For example, increasing d from 0 to 0.5 nm, at p = 4 bars, increases the excess adsorption by 250%, 79%, and 32% for $2r$ = 1, 3, and 8 nm, respectively. The increased adsorption behavior for d = 0.5 nm is mainly attributed to the increased volume of the groove region. The relative volume available in the groove and interstitial regions decreases with increase in the diameter. Hence, the adsorption capacity also follows the same order.

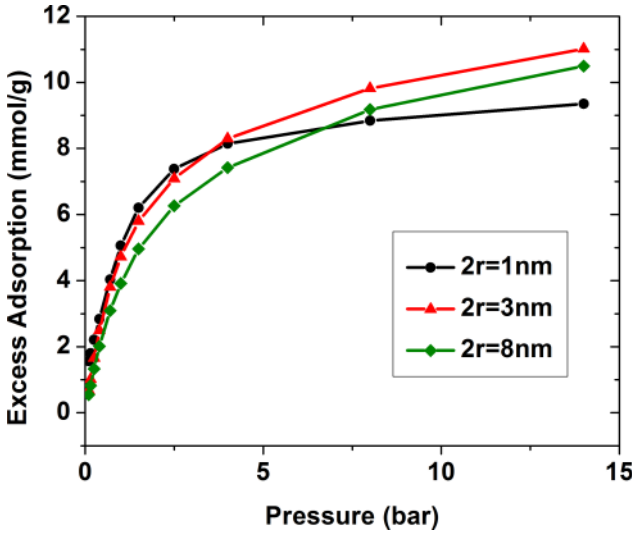

FIG. 5. Excess adsorption isotherms of CO_2 in double-walled carbon nanotube arrays, with intertube distance d = 0.5 nm and inner tube diameter $2r$ = 1-8 nm. T = 303 K. Error bars are smaller than the symbols.

Fig. 5 shows the effect of inner diameter of DWCNT on CO_2 adsorption isotherm with a fixed intertube distance of d = 0.5 nm. At $p < 4$ bars, the excess adsorption of $2r$ = 1 nm is slightly more than that of $2r$ = 3 nm (the maximum difference is 0.4 mmol/g at p = 1.5 bars). The reason is probably the higher curvature of $2r$ = 1 nm compared to that of $2r$ = 3 nm. However, CO_2 adsorption on $2r$ = 1 nm DWCNT saturates quickly with increasing pressure, $p \sim 4$ bars, due to its limited space. At $p > 4$ bars, $2r$ = 3 nm displays the highest excess adsorption so that at p = 14 bars the excess adsorption of it is 1.66 mmol/g more than that of d = 0. Moreover, $2r$ = 3 nm does not saturate within 14 bars. Further increase in the inner diameter decreases the excess adsorption marginally, as seen for $2r$ = 8 nm in the pressure range studied in this work,

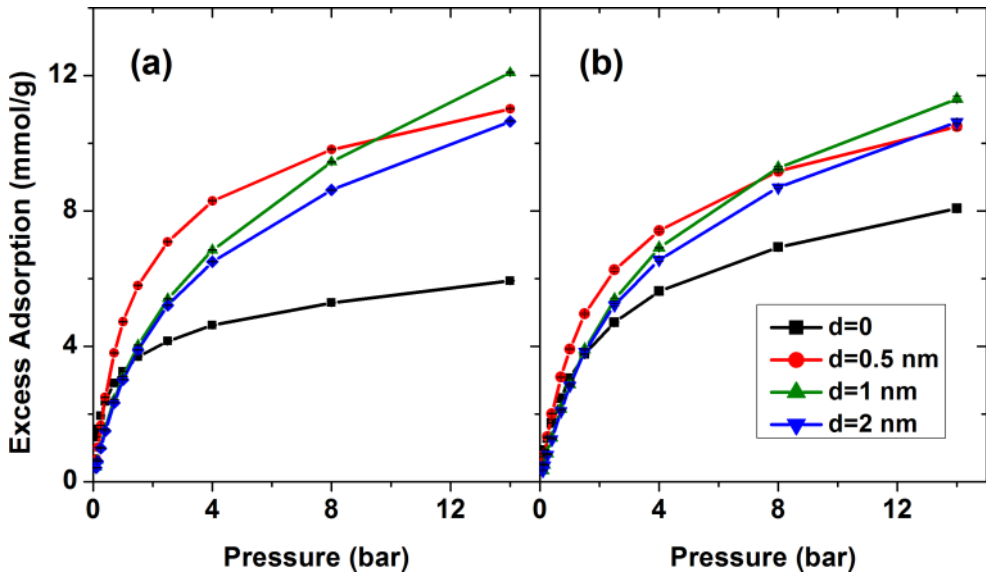

FIG. 4. Excess adsorption isotherms of CO_2 in double-walled carbon nanotube arrays, with inner tube diameter (a) $2r$ = 3 nm, (b) $2r$ = 8 nm and intertube distance d = 0-2 nm. T = 303 K. Error bars are smaller than the symbols.

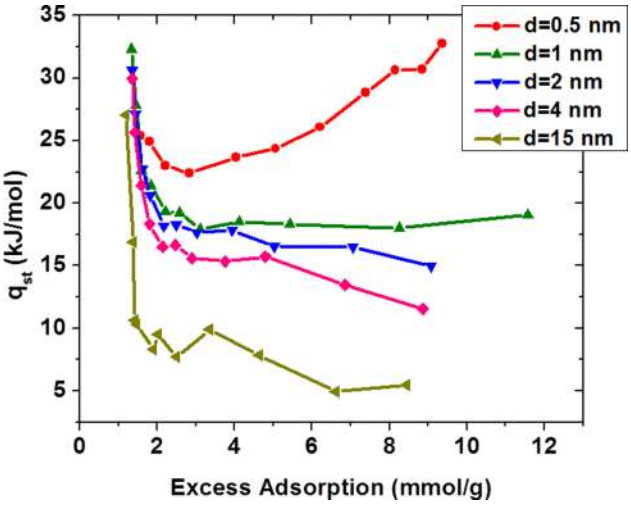

FIG. 6. Isosteric heat of adsorption of CO_2 in double-walled carbon nanotube arrays, with inner tube radius $2r = 1$ nm and intertube distance $d = 0$-15 nm. $T = 303$ K.

because of the reduction in its curvature. It is evident from Fig. 5 that CNT pore diameter has much less effect on the adsorption behavior as compared to the intertube distance (as seen in Figs. 3 and 4).

Fig. 6 presents the heat of adsorption of the systems with $2r = 1$ nm and $d = 0.5$-15 nm as a function of excess adsorption. The heat of adsorption of $d = 0$ is not shown since the excess adsorption of it is almost constant at ~40 kJ/mol. When $d = 0.5$ nm, the heat of adsorption decreases first with increasing excess adsorption until it reaches to a minimum and then it further increases. The initial decrease in q_{st} is due to the filling of grooves, which have a high carbon density. By filling the grooves, followed by the interstitial and the inner regions, which are all very low in volume, q_{st} starts increasing. For higher d, similar to $d = 0.5$ nm, a drastic decrease in q_{st} is seen first while grooves get filled. Subsequently, q_{st} continues to decrease though not dramatically. This is mainly attributed to the continuous filling process of the interstitial and inner volume until saturation. $d = 1$ nm case is an exception where q_{st} remains constant at 18 kJ/mol after the initial drop.

Having high adsorption is not the only main goal, since it is important to have low q_{st} for economically reusable adsorbent for CO_2. Moreover, an optimal CNT array depends on the pressure. For example, for $p = 1$ bar, $2r = 1$ nm and $d = 0.5$ nm is the best material which has the excess adsorption of 5.06 mmol/g (e.g., the excess adsorption is 2.5 and 4.7 mmol/g for $2r = 1$ nm, $d = 1$ nm and $2r = 3$ nm, $d = 0.5$ nm, respectively), though with a high q_{st} of 24 kJ/mol. The lowest q_{st}, 9.52 kJ/mol, belongs to the case with $2r = 1$ nm and $d = 15$ nm which has also the lowest amount of excess adsorption ($N_{ex} = 2.01$ mmol/g). At a higher pressure, e.g., $p = 14$ bars, the case with $2r = 3$ nm and $d = 1$ nm shows the highest adsorption ($N_{ex} = 12.08$ mmol/g) but with $q_{st} = 17.69$ kJ/mol, while the lowest q_{st} is 5.46 kJ/mol (belongs to the case with $2r = 1$ nm and $d = 15$ nm) but with 43% less in adsorption capacity. Hence, clearly there is a trade-off in the amount of adsorption and energy required for reusability.

C. Molecular simulation of SO_2 adsorption

SO_2 isotherms on DWCNT with $2r = 1$, 3, 5, 8 nm and $d = 0$-2 nm at $T = 303$ K are shown in Fig. 7. The system with

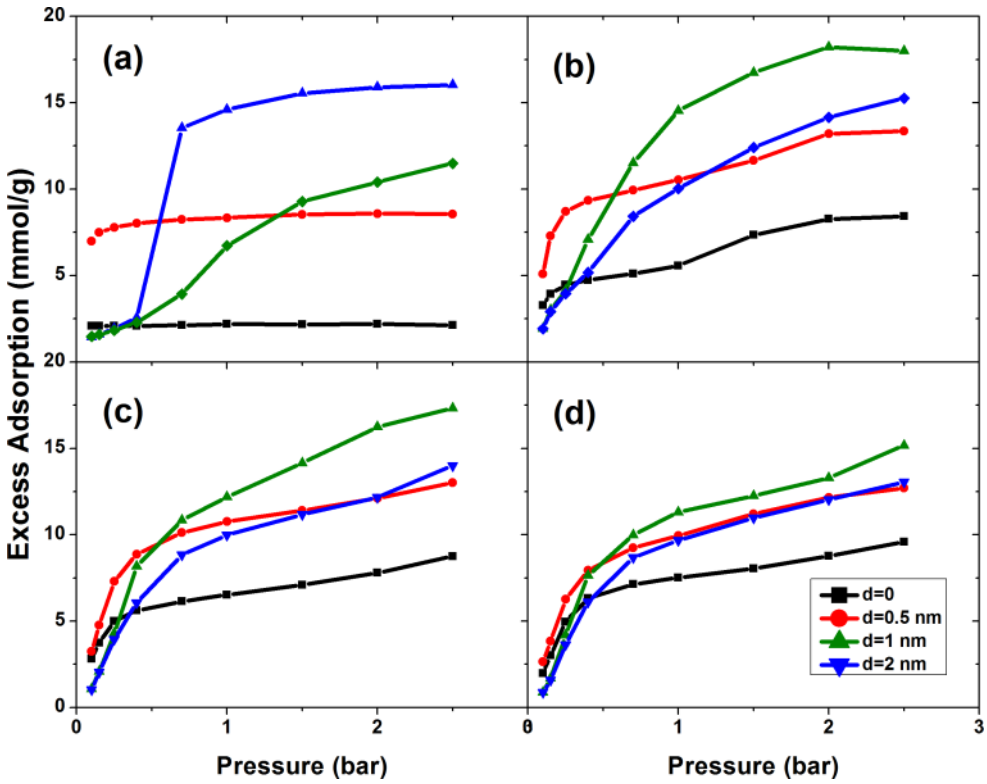

FIG. 7. Excess adsorption isotherms of SO_2 in double-walled carbon nanotube arrays, with inner tube diameter (a) $2r = 1$ nm, (b) $2r = 3$ nm, (c) $2r = 5$ nm, (d) $2r = 8$ nm and intertube distance $d = 0$-2 nm. $T = 303$ K. Error bars are smaller than the symbols.

$2r$ = 1 nm and d = 0 (Fig. 7(a)) shows a low constant excess adsorption in the whole pressure range, because of the limited volume both inside the CNTs and in the intertube region. The case of d = 0.5 nm shows a similar result but with higher amount of adsorption. For d = 1 nm, the amount of adsorption is less than that of d = 0.5 nm for $p < 0.5$ bars. However, at $p \sim 0.5$ bars, the system undergoes capillary condensation. Subsequently, at $p > 0.5$ bars, the amount of adsorption is above that of d = 0.5 nm. Further increase in d to 2 nm yields lower adsorption in the whole pressure range in comparison with d = 1 nm. Furthermore, capillary condensation is not observed for d = 2 nm up to p = 3 bars. Increasing the diameter to 3-8 nm does not change the optimal intertube distance for the highest adsorption capacity. So at very low pressures, $p < 0.5$ bars, d = 0.5 nm has the highest adsorption capacity while at higher pressures, $0.5 < p < 3$, d = 1 nm shows the maximum adsorption capacity. Nevertheless, the effect of d is more dramatic at low CNT diameter.

The optimum intertube distance for the maximum SO_2 adsorption is the same as that for CO_2. However, corresponding pressures are 9 bars and 0.5 bars for CO_2 and SO_2, respectively. Furthermore, the effect of intertube distance is stronger for SO_2 than CO_2. For the case of SO_2, increasing d from 0 to 0.5 nm at p = 1 bar increases the adsorption by 280%, 89%, 65%, and 32% for $2r$ = 1, 3, 5, and 8 nm, respectively. A similar dependence was seen at p = 4 bars for the case of CO_2. This is due to the stronger interaction of SO_2 molecules with the CNT and also with each other. Fig. S4[40] shows the CO_2 and SO_2 isotherms for $2r$ = 3 nm and d = 0-2 nm, which clearly indicate higher adsorption for SO_2 than that for CO_2 under the same condition.

In the case of $2r$ = 3 nm and d = 0 (Fig. 7(b)), a primary increase in the adsorption is seen, as the pressure is increased till p = 0.3 bars. Then, for 0.3 bars < p < 1 bar, the adsorption increases gradually. Further increase in pressure enhances the adsorption distinctly, as seen in the second increase in the adsorption curve between 1 bar and 2 bars. This can be explained due to the layering transition. The snapshots of the system are shown in Fig. 8. When d = 0, the groove and interstitial regions have very limited capacity and are saturated at a low pressure $p \sim 0.1$ bars. Inside the CNT, the first layer of adsorption is formed at $p \sim 0.2$ bars. By increasing the pressure to 1 bar, the first layer slowly saturates indicated by the slow increase in the adsorption isotherm. By further increase in pressure, the second layer starts to form. Formation of the second layer causes saturation in the inner space, which is reflected in the significant increase in the adsorption isotherm value. The same situation is found for d = 0.5 nm. For d = 1 nm, the inner and outer regions are saturated almost at the same pressure. Hence, the curve has a continuous increase in the whole pressure range, and the layering transition is not seen. The curve of d = 2 nm is similar to d = 1 nm because groove and interstitial regions are not completely filled below 3 bars. The adsorption isotherm displays no rapid increase

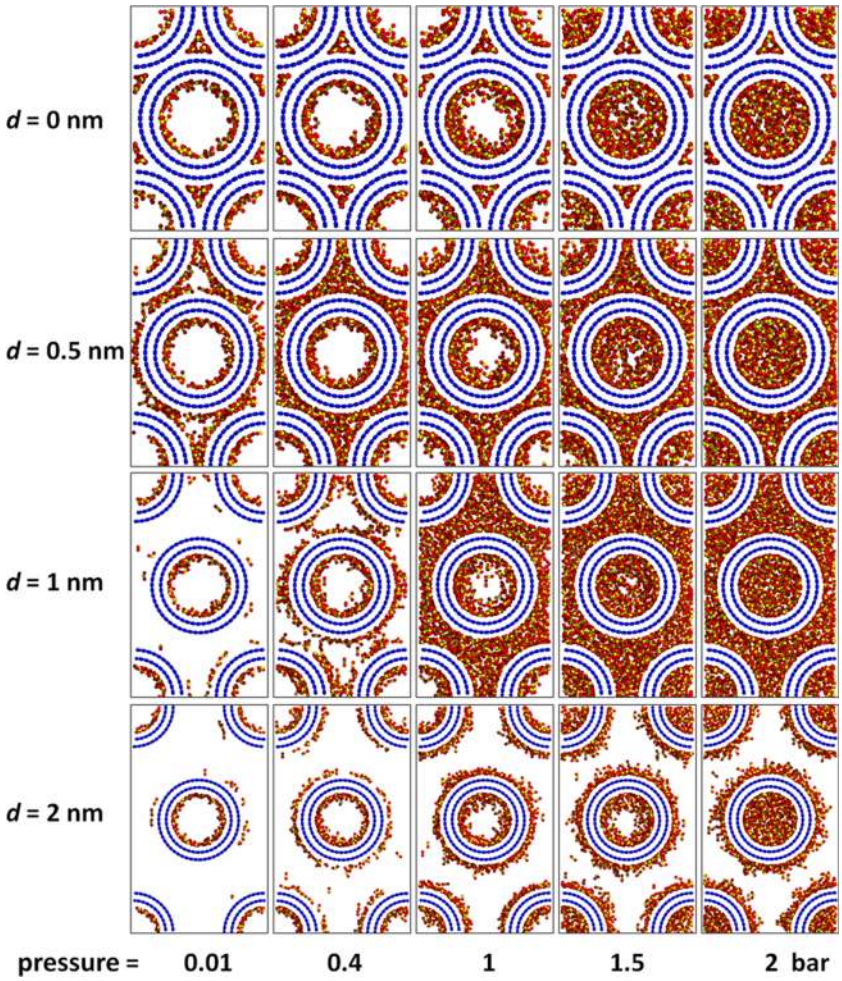

FIG. 8. Snapshots of SO_2 adsorption in double-walled carbon nanotube arrays, with inner tube diameter $2r$ = 3 nm and various intertube distances. T = 303 K.

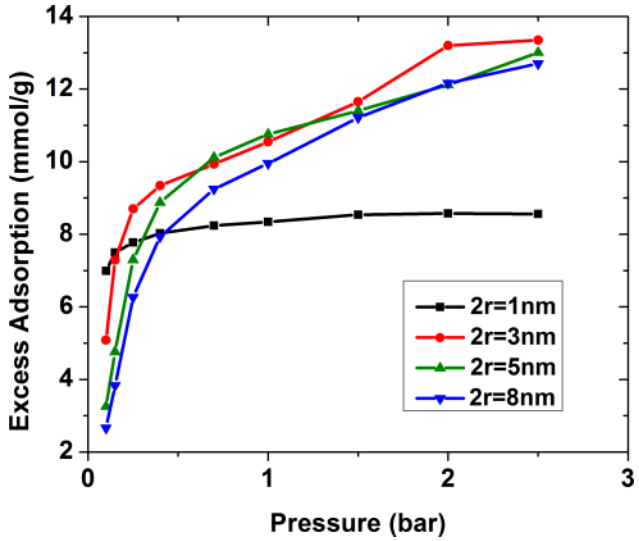

FIG. 9. Excess adsorption isotherms of SO_2 in double-walled carbon nanotube arrays, with intertube distance $d = 0.5$ nm and inner tube diameter $2r = 1$-8 nm. $T = 303$ K. Error bars are smaller than the symbols.

change of curvature for thicker CNTs. The reason is possibly the larger available space inside the CNTs, for which the transition from first layer to second layer does not lead to saturation inside the CNT.

Fig. 9 presents SO_2 isotherm on double-walled CNT of varying diameters at a fixed intertube distance of $d = 0.5$ nm. As for CO_2, the effect of diameter is not as dramatic as that of the intertube distance. For $2r = 1$ nm, the adsorption is almost constant due to the limited available space, inside and outside of the CNT, in comparison with the SO_2 molecular size. The case with $2r = 3$ nm has the highest adsorption in the whole pressure range except 0.6 bars $< p <$ 1.2 bars. This exception is due to the layering transition explained above. Larger tube curvature leads to higher adsorption but at the same time having enough volume is an important factor too. In the studied pressure range, CNTs with $2r = 3$ nm are the best compromise of high curvature with sufficient volume at the same time.

Langmuir and Freundlich models have also been fitted to the SO_2 adsorption data of the system with $2r = 3$ nm and various d values. Table II summarizes the fitted model parameters. For the Langmuir model, $d = 1$ nm has the highest capacity for SO_2 adsorption so that N_{ex}^{max} of $d = 1$ nm is 100% and 19% more than that of $d = 0.5$ and 2 nm, respectively. For the Freundlich model, $d = 1$ nm shows a value of K of $d = 1$ nm 12% and 29% more than that of $d = 0.5$ and $d = 2$ nm, respectively. Similar to the case of CO_2, the optimal CNT intertube distance and diameter for SO_2 adsorption depend on the pressure. For instance, at $p = 1$ bar, the system with $2r = 1$ nm and $d = 1$ nm is found to have the highest adsorption while the case with $2r = 3$ nm and $d = 1$ nm leads to maximum adsorption at $p = 2.5$ bars.

TABLE II. Langmuir and Freundlich isotherm parameters obtained by fitting the SO_2 adsorption data on double-walled CNT with $2r = 3$ nm and $d = 0$-2 nm. R^2 is the coefficient of determination of fitting.

	Langmuir model			Freundlich model		
d	N_{ex}^{max}	b	R^2	K	n	R^2
0	8.37 ± 0.71	4.27 ± 1.40	0.78	6.33 ± 0.16	0.30 ± 0.03	0.94
0.5	13.25 ± 0.54	6.60 ± 1.21	0.96	10.89 ± 0.24	0.24 ± 0.02	0.94
1	27.16 ± 2.10	0.97 ± 0.17	0.98	12.25 ± 0.67	0.55 ± 0.67	0.93
2	22.65 ± 0.73	0.82 ± 0.06	0.99	9.46 ± 0.23	0.57 ± 0.031	0.99

V. CONCLUSION

In this work, molecular simulation and experiments were used to find a geometry for three-dimensionally aligned double-walled CNT arrays, which is optimum for having higher CO_2 and SO_2 adsorption at low pressures and $T = 303$ K. Experimental results for CO_2 adsorption on CNT with inner diameter of 8 nm show that reducing the intertube distance leads to increase in adsorption at $p = 1$ bar. Molecular simulation investigations were performed on double-walled CNTs with inner diameters 1-8 nm and intertube distances of 0-15 nm. The results show that for CO_2 adsorption at low pressure, $p < 9$ bars, the $d = 0.5$ nm system has the highest adsorption, while for the pressure range $9 < p < 14$ bars, the maximum adsorption is found for $d = 1$ nm. Reducing the intertube distance from $d = 2$ to $d = 0.5$ nm at $p = 1$ bar increases the adsorption capacity by 103, 57, 46, and 38% for $2r = 1$, 3, 5, and 8 nm, respectively. On the other hand, the experimental results of CO_2 adsorption show an increase of 34% and 57% for CNT architectures, which have been compacted by ethanol and water treatment, respectively, for $2r = 8$ nm at $p = 1$ bar. Although the experiments and simulation results do not give the same value, the results are in line with each other qualitatively.

For SO_2 adsorption, the optimal intertube distances are akin to those seen for CO_2; however, the pressure, where crossover occurs, is much lower at ~0.5 bars. Furthermore, it was found that the intertube distance has a much larger effect on gas adsorption than the tube diameter. As a result, the optimal CNT geometry depends on the operating pressure and the gas. For example, at $p = 1$ bar, DWCNTs with $2r = 1$ nm and $d = 0.5$ nm show the highest adsorption capacity for CO_2, while $2r = 3$ nm and $d = 1$ nm show the maximum adsorption capacity for SO_2.

ACKNOWLEDGMENTS

D.J.B. and J.J.S. would like to thank Silvio Heinschke for the N_2 adsorption measurement. M.R. would like to thank Jurek Schneider for his help in free volume calculations. This work was supported by the Priority Programme 1570 *Porous media with well-defined pore structure in chemical engineering: Modelling, application, synthesis* of Deutsche Forschungsgemeinschaft. J.K.S. gratefully acknowledges the support of the Alexander von Humboldt Foundation, and the Ministry of Earth Sciences, India.

[1]R. K. Pachauri, M. R. Allen, V. R. Barros, J. Broome, W. Cramer, R. Christ, J. A. Church, L. Clarke, Q. Dahe, P. Dasgupta, N. K. Dubash, O. Edenhofer, I. Elgizouli, C. B. Field, P. Forster, P. Friedlingstein, J. Fuglestvedt, L. Gomez-Echeverri, S. Hallegatte, G. Hegerl, M. Howden, K. Jiang, B. Jimenez Cisneros, V. Kattsov, H. Lee, K. J. Mach, J. Marotzke, M. D. Mastrandrea, L. Meyer, J. Minx, Y. Mulugetta, K. O'Brien, M. Oppenheimer, J. J. Pereira,

R. Pichs-Madruga, G.-K. Plattner, H.-O. Pörtner, S. B. Power, B. Preston, N. H. Ravindranath, A. Reisinger, K. Riahi, M. Rusticucci, R. Scholes, K. Seyboth, Y. Sokona, R. Stavins, T. F. Stocker, P. Tschakert, D. van Vuuren, and J.-P. van Ypersele, IPCC, 2014: *Climate Change 2014: Synthesis Report. Contribution of Working Groups I, II and III to the Fifth Assessment Report of the Intergovernmental Panel on Climate Change*, edited by R. Pachauri and L. Meyer (IPCC, Geneva, Switzerland), 151 pp., http://hdl.handle.net/10013/epic.45156.

[2]D. M. D'Alessandro, B. Smit, and J. R. Long, "Carbon dioxide capture: Prospects for new materials," Angew. Chem., Int. Ed. **49**, 6058–6082 (2010).

[3]A. D. Ellerman, *Markets for Clean Air: The U.S. Acid Rain Program* (Cambridge University Press, 2000).

[4]F. L. Darkrim, P. Malbrunot, and G. P. Tartaglia, "Review of hydrogen storage by adsorption in carbon nanotubes," Int. J. Hydrogen Energy **27**, 193–202 (2002).

[5]M. J. O'Connell, *Carbon Nanotubes: Properties and Applications* (CRC Press, 2006).

[6]X. Ren, C. Chen, M. Nagatsu, and X. Wang, "Carbon nanotubes as adsorbents in environmental pollution management: A review," Chem. Eng. J. **170**, 395–410 (2011).

[7]E. J. Bottani and J. M. D. Tascón, *Adsorption by Carbons: Novel Carbon Adsorbents* (Elsevier, 2011).

[8]A. V. Eletskii, "Sorption properties of carbon nanostructures," Phys.-Usp. **47**, 1119–1154 (2004).

[9]L. Liu and S. K. Bhatia, "Molecular simulation of CO_2 adsorption in the presence of water in single-walled carbon nanotubes," J. Phys. Chem. C **117**, 13479–13491 (2013).

[10]X. Peng, D. Cao, and W. Wang, "Adsorption and separation of $CH_4/CO_2/N_2/H_2/CO$ mixtures in hexagonally ordered carbon nanopipes CMK-5," Chem. Eng. Sci. **66**, 2266–2276 (2011).

[11]P. Kowalczyk, S. Furmaniak, P. A. Gauden, and A. P. Terzyk, "Optimal single-walled carbon nanotube vessels for short-term reversible storage of carbon dioxide at ambient temperatures," J. Phys. Chem. C **114**, 21465–21473 (2010).

[12]A. Cao, H. Zhu, X. Zhang, X. Li, D. Ruan, C. Xu, B. Wei, J. Liang, and D. Wu, "Hydrogen storage of dense-aligned carbon nanotubes," Chem. Phys. Lett. **342**, 510–514 (2001).

[13]D. Zilli, P. R. Bonelli, and A. L. Cukierman, "Effect of alignment on adsorption characteristics of self-oriented multi-walled carbon nanotube arrays," Nanotechnology **17**, 5136–5141 (2006).

[14]S. Agnihotri, J. P. B. Mota, M. Rostam-Abadi, and M. J. Rood, "Structural characterization of single-walled carbon nanotube bundles by experiment and molecular simulation," Langmuir **21**, 896–904 (2005).

[15]F. J. A. L. Cruz, I. A. A. C. Esteves, and J. P. B. Mota, "Adsorption of light alkanes and alkenes onto single-walled carbon nanotube bundles: Langmuirian analysis and molecular simulations," Colloids Surf., A **357**, 43–52 (2010).

[16]W. Shi and J. Johnson, "Gas adsorption on heterogeneous single-walled carbon nanotube bundles," Phys. Rev. Lett. **91**, 015504 (2003).

[17]S. Agnihotri, J. P. B. Mota, M. Rostam-Abadi, and M. J. Rood, "Adsorption site analysis of impurity embedded single-walled carbon nanotube bundles," Carbon **44**, 2376–2383 (2006).

[18]F. J. A. L. Cruz, I. A. A. C. Esteves, S. Agnihotri, and J. P. B. Mota, "Adsorption equilibria of light organics on single-walled carbon nanotube heterogeneous bundles: Thermodynamical aspects," J. Phys. Chem. C **115**, 2622–2629 (2011).

[19]J. J. Cannon, T. J. H. Vlugt, D. Dubbeldam, S. Maruyama, and J. Shiomi, "Simulation study on the adsorption properties of linear alkanes on closed nanotube bundles," J. Phys. Chem. B **116**, 9812–9819 (2012).

[20]F. Cruz and J. Mota, "Thermodynamics of adsorption of light alkanes and alkenes in single-walled carbon nanotube bundles," Phys. Rev. B **79**, 165426 (2009).

[21]M. Rahimi, J. K. Singh, D. J. Babu, J. J. Schneider, and F. Müller-Plathe, "Understanding carbon dioxide adsorption in carbon nanotube arrays: Molecular simulation and adsorption measurements," J. Phys. Chem. C **117**, 13492–13501 (2013).

[22]D. J. Babu, M. Lange, G. Cherkashinin, A. Issanin, R. Staudt, and J. J. Schneider, "Gas adsorption studies of CO_2 and N_2 in spatially aligned double-walled carbon nanotube arrays," Carbon **61**, 616–623 (2013).

[23]R. Joshi, J. Engstler, L. Houben, M. B. Sadan, A. Weidenkaff, P. Mandaliev, A. Issanin, and J. J. Schneider, "Catalyst composition, morphology and reaction pathway in the growth of 'super-long' carbon nanotubes," ChemCatChem **2**, 1069–1073 (2010).

[24]J. G. Harris and K. H. Yung, "Carbon dioxide's liquid-vapor coexistence curve and critical properties as predicted by a simple molecular model," J. Phys. Chem. **99**, 12021–12024 (1995).

[25]M. H. Ketko, G. Kamath, and J. J. Potoff, "Development of an optimized intermolecular potential for sulfur dioxide," J. Phys. Chem. B **115**, 4949–4954 (2011).

[26]W. D. Cornell, P. Cieplak, C. I. Bayly, I. R. Gould, K. M. Merz, D. M. Ferguson, D. C. Spellmeyer, T. Fox, J. W. Caldwell, and P. A. Kollman, "A second generation force field for the simulation of proteins, nucleic acids, and organic molecules," J. Am. Chem. Soc. **117**, 5179–5197 (1995).

[27]U. Essmann, L. Perera, M. L. Berkowitz, T. Darden, H. Lee, and L. G. Pedersen, "A smooth particle mesh Ewald method," J. Chem. Phys. **103**, 8577 (1995).

[28]M. L. Greenfield and D. N. Theodorou, "Geometric analysis of diffusion pathways in glassy and melt atactic polypropylene," Macromolecules **26**, 5461–5472 (1993).

[29]J. Jiang and S. I. Sandler, "Separation of CO_2 and N_2 by adsorption in C_{168} schwarzite: A combination of quantum mechanics and molecular simulation study," J. Am. Chem. Soc. **127**, 11989–11997 (2005).

[30]R. Babarao, Z. Hu, J. Jiang, S. Chempath, and S. I. Sandler, "Storage and separation of CO_2 and CH_4 in silicalite, C_{168} schwarzite, and IRMOF-1: A comparative study from Monte Carlo simulation," Langmuir **23**, 659–666 (2007).

[31]D. J. Babu, S. Yadav, T. Heinlein, G. Cherkashinin, and J. J. Schneider, "Carbon dioxide plasma as a versatile medium for purification and functionalization of vertically aligned carbon nanotubes," J. Phys. Chem. C **118**, 12028–12034 (2014).

[32]D. J. Babu, S. N. Varanakkottu, A. Eifert, D. de Koning, G. Cherkashinin, S. Hardt, and J. J. Schneider, "Inscribing wettability gradients onto superhydrophobic carbon nanotube surfaces," Adv. Mater. Interfaces **1**, 1300049 (2014).

[33]T. Yamada, T. Namai, K. Hata, D. N. Futaba, K. Mizuno, J. Fan, M. Yudasaka, M. Yumura, and S. Iijima, "Size-selective growth of double-walled carbon nanotube forests from engineered iron catalysts," Nat. Nanotechnol. **1**, 131–136 (2006).

[34]B. Zhao, D. N. Futaba, S. Yasuda, M. Akoshima, T. Yamada, and K. Hata, "Exploring advantages of diverse carbon nanotube forests with tailored structures synthesized by supergrowth from engineered catalysts," ACS Nano **3**, 108–114 (2009).

[35]M. De Volder and A. J. Hart, "Engineering hierarchical nanostructures by elastocapillary self-assembly," Angew. Chem., Int. Ed. **52**, 2412–2425 (2013).

[36]D. N. Futaba, K. Hata, T. Yamada, T. Hiraoka, Y. Hayamizu, Y. Kakudate, O. Tanaike, H. Hatori, M. Yumura, and S. Iijima, "Shape-engineerable and highly densely packed single-walled carbon nanotubes and their application as super-capacitor electrodes," Nat. Mater. **5**, 987–994 (2006).

[37]H.-J. Butt, K. Graf, and M. Kappl, *Physics and Chemistry of Interfaces* (John Wiley & Sons, 2006).

[38]I. Langmuir, "The adsorption of gases on plane surfaces of glass, mica and platinum," J. Am. Chem. Soc. **40**, 1361–1403 (1918).

[39]H. Freundlich, *Kapillarchemie* (Akademische Verlagsgesellschaft, Wiesbaden, Germany, 1909).

[40]See supplementary material at http://dx.doi.org/10.1063/1.4929609 for the simulation data, best, and worst fits of Langmuir and Freundlich of excess adsorption isotherms of CO_2 in double-walled carbon nanotube arrays.